Forensic Toxicol (2017) 35:20–32
DOI 10.1007/s11419-016-0326-9

ORIGINAL ARTICLE

In vitro and in vivo human metabolism of a new synthetic cannabinoid NM-2201 (CBL-2201)

Xingxing Diao[1] · Jeremy Carlier[1] · Mingshe Zhu[2] · Shaokun Pang[3] · Robert Kronstrand[4,5] · Karl B. Scheidweiler[1] · Marilyn A. Huestis[1,6]

Received: 19 May 2016 / Accepted: 13 June 2016 / Published online: 6 July 2016

Abstract In 2014, NM-2201 (CBL-2201), a novel synthetic cannabinoid (SC), was detected by scientists at Russian and US laboratories. It has been already added to the list of scheduled drugs in Japan, Sweden and Germany. Unfortunately, no human metabolism data are currently available, which makes it challenging to confirm its intake, especially given that all SCs investigated thus far have been found to be extensively metabolized. The present study aims to recommend appropriate marker metabolites by investigating NM-2201 metabolism in human hepatocytes, and to confirm the results in authentic human urine specimens. For the metabolic stability assay, 1 μM NM-2201 was incubated in human liver microsomes (HLMs) for up to 1 h; for metabolite profiling, 10 μM of NM-2201 was incubated in human hepatocytes for 3 h. Two authentic urine specimens from NM-2201-positive cases were subjected to β-glucuronidase hydrolysis prior to analysis. The identification of metabolites in hepatocyte samples and urine specimens was achieved with high-resolution mass spectrometry via information-dependent acquisition. NM-2201 was quickly metabolized in HLMs, with an 8.0-min half-life. In human hepatocyte incubation samples, a total of 13 NM-2201 metabolites were identified, generated mainly from ester hydrolysis and further hydroxylation, oxidative defluorination and subsequent glucuronidation. M13 (5-fluoro PB-22 3-carboxyindole) was found to be the major metabolite. In the urine specimens, the parent drug NM-2201 was not detected; M13 was the predominant metabolite after β-glucuronidase hydrolysis. Therefore, based on the results of our study, we recommend M13 as a suitable urinary marker metabolite for confirming NM-2201 and/or 5F-PB-22 intake.

Keywords NM-2201 · CBL-2201 · Synthetic cannabinoid · In vitro human hepatocyte metabolism · High-resolution mass spectrometry · Authentic human urine specimen

✉ Karl B. Scheidweiler
kscheidweiler@intra.nida.nih.gov

1 Chemistry and Drug Metabolism Section, Clinical Pharmacology and Therapeutics Branch, Intramural Research Program, National Institute on Drug Abuse, National Institutes of Health, 251 Bayview Blvd, Suite 200 Room 05A727, Baltimore, MD 21224, USA

2 Department of Biotransformation, Bristol-Myers Squibb, Research and Development, Princeton, NJ 08543, USA

3 SCIEX, Redwood City, CA 94065, USA

4 Department of Forensic Genetics and Forensic Toxicology, National Board of Forensic Medicine, 58758 Linköping, Sweden

5 Department of Drug Research, University of Linköping, 58185 Linköping, Sweden

6 University of Maryland School of Medicine, Baltimore, MD 21224, USA

Introduction

Since the first report in 2008, the abuse of synthetic cannabinoids (SCs) as recreational drugs for their psychoactive effects, generally through smoking/inhalation, has become increasingly common [1, 2]. Initially developed as pharmacological probes for investigating the endocannabinoid system and developing potential therapeutic compounds [3, 4], many SCs and their metabolites possess higher binding affinity to cannabinoid receptor 1 (CB_1) and CB_2 than conventional cannabinoids such as Δ^9-tetrahydrocannabinol, producing greater cannabinoid receptor-mediated effects in the central and peripheral

nervous systems [5]. Novel psychoactive substances (NPSs) are manufactured at clandestine chemical laboratories, and generally emerge in Europe or Japan before they are identified in the United States [6]. Abuse of these SCs can result in severe toxic effects including psychotic episodes, kidney failure, acute cerebral ischemia, myocardial infarction and even death [7–10]. Dependence on these compounds can develop, especially with daily SC intake [11]. For these reasons, SCs have been added to scheduled drug lists in many countries, including the European Union countries, the United States, China, Japan, Russia and Australia [6, 12].

As a means of skirting regulations, more structurally diverse analogs are continually being released into the illegal drug market. In Japan, as of April 2015, a total of 858 SCs were scheduled as narcotics or designated substances [13]. In addition to structural analogs, a new trend is forming, with positional isomers now appearing on the illegal drug market. For instance, THJ-2201 was scheduled in the United States in February 2015 and in Japan in August 2014; its positional isomer, FUBIMINA (BIM-2201), quickly emerged and became popular among drug users. FUBIMINA and THJ-2201 shared the same metabolic pathway, and their major metabolites were also pairs of isomers, making it difficult to distinguish their intake [14]. This new phenomenon creates further challenges in confirming the specific SC consumed. In most cases, the detailed pharmacological activity of these SCs is unknown and unpredictable, making their easy access and uncontrolled dissemination a serious threat to public health and safety. Potential drug-drug interactions may increase adverse effects when metabolic pathways are altered with simultaneous intake of multiple synthetic drugs [15]. In some SCs, human metabolism leads to differential pharmacodynamic and pharmacokinetic properties, and may produce clinical toxicity such as that which occurred with JWH-018 and AM-2201 [16].

NM-2201 [naphthalen-1-yl 1-(5-fluoropentyl)-1*H*-indole-3-carboxylate], also known as CBL-2201, is a recently emerging SC (Fig. 1a). NM-2201 is structurally similar to 5F-PB-22 (Fig. 1b), with the only difference being the naphthalene or quinoline ring, respectively, connected to the *N*-fluoropentyl indole core via an ester bond. Compared to AM-2201 (Fig. 1c), the linkage between naphthalene and the indole core in NM-2201 changed from the carbonyl to the ester. The US Army Criminal Investigation Laboratory (USACIL) first reported positive NM-2201 cases in October 2014 (unpublished data), and NM-2201 was detected by Russian researchers in 2014 and 2015 [17, 18]. Proliferation of NPSs is a global challenge; identifying NPS intake and linking specific adverse effects to causative agents requires rapid elucidation of the NPSs and their major urinary metabolites, as SCs are typically extensively

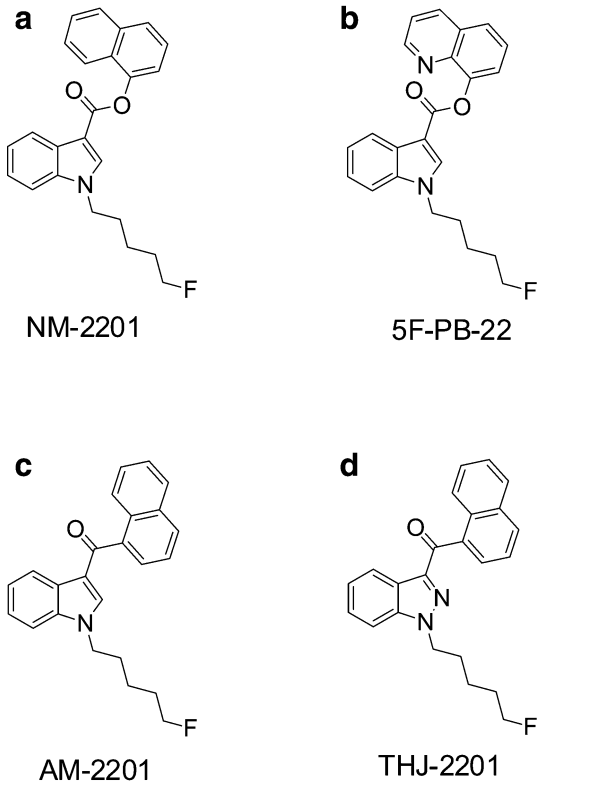

Fig. 1 Structures of synthetic cannabinoids NM-2201 (**a**), 5F-PB-22 (**b**), AM-2201 (**c**), and THJ-2201 (**d**)

metabolized, and the parent drug is rarely present in urine [17, 19, 20]. To the best of our knowledge, there are no clinical studies investigating the pharmacological and toxicological effects and pharmacokinetics of NM-2201. What little data that are available are found on Internet drug user forums—for instance, www.drug-forum.com, www.bluelight.org. Drug users reported that NM-2201 was potent but did not last as long as JWH-018 [21]. Caution is warranted when inferring pharmacologic effects, however, since drug users are frequently unaware of what compounds they are actually ingesting.

All SCs investigated to date are extensively metabolized in humans and are predominantly excreted as metabolites in urine [6, 16, 22, 23], complicating detection, as metabolites are initially unknown. Knowledge of human metabolism is critical for verifying NM-2201 consumption, since urine testing is routine for workplace, clinical and forensic testing. Unfortunately, controlled human pharmacokinetics studies are not yet possible due to the lack of pharmacology, toxicity and safety data for SCs. Although there are no published data for NM-2201, in vitro metabolism studies of their analogs 5F-PB-22 and AM-2201 are available [12, 22]. 5F-PB-22 was subjected to extensive ester hydrolysis, followed by oxidative defluorination [12], but no human urine samples were studied to confirm the

hepatocyte results. For AM-2201, oxidative defluorination with subsequent carboxylation and glucuronidation is the primary metabolic pathway [22]. It is not known whether the minor structural change from 5F-PB-22 or AM-2201 to NM-2201 alters the metabolic profile.

In the present study, we evaluated the metabolic stability of NM-2201 in human liver microsomes (HLMs), and then incubated NM-2201 in human hepatocytes for metabolite profiling. Hepatocytes are superior to HLMs for metabolite profiling because they better mimic the physiological environment [24, 25]. Our previous human hepatocyte metabolism studies have proven the success of the hepatocyte incubation model for identifying appropriate marker metabolites including AB-FUBINACA [26], AB-PINACA [20], FDU-PB-22 and FUB-PB-22 [27]. Two urine samples collected from individuals suspected of driving under the influence of drugs were also investigated. Metabolite elucidation was achieved with high-performance liquid chromatography (HPLC) coupled with the TripleTOF 5600+ quadrupole/time-of-flight high-resolution mass spectrometer (HR-MS; AB SCIEX, Framingham, MA, USA). Human hepatocyte metabolites were compared to urinary metabolites, and the optimal metabolites for determining NM-2201 intake were identified.

Our goal was to investigate in vitro human metabolism of NM-2201 and to confirm marker metabolites in authentic urine specimens. The identified optimal urinary markers could thus be incorporated into screening methods for documenting SC intake, linking adverse events with the causative substances, and providing reference standard manufacturers with the most critical metabolites for their synthesis efforts.

Materials and methods

Chemicals and reagents

NM-2201 (95.92 % pure) was kindly provided by the Special Testing and Research Laboratory (Dulles, VA, USA), US Drug Enforcement Administration, US Department of Justice. 5-Fluoro PB-22 3-carboxyindole metabolite (5F-PI-COOH, ≥98 %), PB-22 *N*-(5-hydroxypentyl)-3-carboxyindole metabolite (5′-OH-PI-COOH, ≥98 %) and PB-22 *N*-pentanoic acid-3-carboxyindole metabolite (PI-COOH pentanoic acid, ≥98 %) were purchased from Cayman Chemical (Ann Arbor, MI, USA); HLMs (50-donor pool), NADPH, 10-donor-pooled cryopreserved human hepatocytes, *InVitro*GRO CP and KHB buffer from BioreclamationIVT (Baltimore, MD, USA); Red Abalone BG100® β-glucuronidase from Kura Biotec (100,000 U/mL, Puerto Varas, Chile); liquid chromatography-mass spectrometry (LC–MS)-grade acetonitrile and ethyl acetate from Sigma-Aldrich (St. Louis, MO, USA); and LC–MS-grade water, acetic acid and formic acid from Fisher Scientific (Waltham, MA, USA). Isolute® SLE+ (1 mL) supported liquid extraction cartridges (Biotage, Charlotte, NC, USA) were used for urine sample extraction.

Metabolic stability assay in HLMs

The metabolic stability of NM-2201 was evaluated in HLM suspensions as described previously, with slight modification [28, 29]. In brief, the HLM incubation mixture contained 50 mM potassium phosphate buffer (pH 7.4), NADPH regenerating system (glucose-6-phosphate, $MgCl_2$, and glucose-6-phosphate dehydrogenase), and 1 μM NM-2201. Incubation was conducted at 37 °C for 1 h in a shaking water bath. The final percentage of organic solvent was <1 %. Samples were collected in 100-μL aliquots at 0, 3, 8, 13, 20, 30, 45 and 60 min, and added to 100 μL ice-cold acetonitrile. The samples were centrifuged (15,000×*g*, 4 °C, 10 min), and the supernatant was then removed and stored at −80 °C. After thawing and vortexing, samples were centrifuged (15,000×*g*, 4 °C, 5 min), 10 μL of supernatant was diluted with 990 μL mobile phase A/B (90: 10, v/v), and 10 μL was injected into the liquid chromatography-tandem mass spectrometry (LC–MS/MS) instrument.

The HPLC system consisted of two LC-20ADXR pumps, a DGU-20A3R degasser, a SIL-20ACXR autosampler and a CTO-20A column oven (Shimadzu Scientific Instruments, Columbia, MD, USA). Chromatography was performed on a Kinetex® C18 column (100 mm × 2.1 mm ID, 2.6 μm) with a KrudKatcher Ultra HPLC in-line filter (0.5 μm × 0.1 mm ID) (Phenomenex Inc., Torrance, CA, USA). Mobile phases were 0.1 % formic acid in water (A) and 0.1 % formic acid in acetonitrile (B); the gradient remained at 10 % B for 0.5 min, was ramped to 95 % B at 10 min, then held until 12.5 min, before re-equilibration at 10 % B for another 2.5 min. Total run time was 15 min at 0.3 mL/min. Column and autosampler temperatures were 40 and 4 °C, respectively.

NM-2201 concentrations in HLM incubation samples were determined on a QTRAP 3200 mass spectrometer (AB SCIEX) via positive electrospray ionization (+ESI). The +ESI source parameters were as follows: source temperature, 500 °C; ion spray voltage, 4000 V; curtain gas, 30 psi; gas 1, 50 psi; gas 2, 50 psi. A pair of multiple reaction monitoring transitions were monitored for NM-2201 (*m/z* 376.2 → 232.2; *m/z* 376.2 → 144.2). Declustering potential was 36 V (target ion, T) and 50 V (qualifier ion, Q); collision energies were 25 eV (T) and 51 eV (Q).

Peak areas of the remaining NM-2201 were plotted versus time points, and microsomal half-life ($T_{1/2}$) and intrinsic clearance ($CL_{int,\ micr}$) were calculated [30].

Intrinsic clearance (CL_{int}) was scaled from microsomal intrinsic clearance in whole-liver dimensions. Human hepatic clearance (CL_H) and extraction ratio (ER) were estimated without considering plasma-protein binding.

Metabolic identification in human hepatocytes

Hepatocyte incubation was performed as previously described [29, 31]. The chemical stability of NM-2201 in incubation buffer also was investigated (37 °C, 3 h) to determine whether metabolite formation was dependent on hepatocyte enzymes. Samples were kept at −80 °C until analysis.

The frozen samples were thawed and vortexed thoroughly. A 100-µL volume of acetonitrile was added to 100 µL sample, and the mixture was vortexed and centrifuged at 15,000×*g* (4 °C, 5 min), and the supernatant transferred to a new tube. After evaporation to dryness under nitrogen at 40 °C, and reconstitution in 150 µL mobile phase A/B (80:20, *v*/*v*), a 15-µL aliquot was injected for analysis.

The HPLC system consisted of two LC-20ADXR pumps, a DGU-20A5R degasser, an SIL-20ACXR autosampler and a CTO-20AC column oven (Shimadzu Scientific Instruments). Chromatographic separation was achieved on an Ultra Biphenyl column (100 mm × 2.1 mm ID, 3 µm; Restek Corp., Bellefonte, PA, USA) equipped with a guard column containing identical packing material. Gradient elution was performed with 0.1 % formic acid in water (A) and 0.1 % formic acid in acetonitrile (B) at 0.5 mL/min. Starting gradient was 20 % B, held for 0.5 min; then increased to 95 % B over 10.5 min, held until 13.0 min; and returned to 20 % B at 13.1 min and held until 15.0 min. HPLC eluent was diverted to MS between 2.0 and 13.0 min. The column oven and autosampler were set at 30 and 4 °C, respectively.

A TripleTOF 5600+ mass spectrometer (AB SCIEX) was used for data acquisition in +ESI mode. MS data were acquired by information-dependent acquisition (IDA) in combination with multiple mass defect filters (MDF) and dynamic background subtraction. The +ESI source parameters were as follows: source temperature, 650 °C; ion spray voltage, 4000 V; gas 1, 60 psi; gas 2, 75 psi; curtain gas, 45 psi; declustering potential, 80 V; collision entrance potential, 10 V. For IDA, spectra exceeding 100 cps were selected for the dependent MS/MS scan, isotopes within 1.5 Da were excluded, and mass tolerance was 50 mDa. Spectra were acquired by scanning a mass range of *m/z* 100–1000, followed by product ion scanning from *m/z* 60 to 1000. The collision energy spread was 35 ± 15 eV. The mass spectrometer was automatically calibrated after every three injections.

Acquired MS data were processed using MetabolitePilot software (version 1.5, AB SCIEX), incorporating different peak-finding algorithms (product ion and neutral loss, MDF, predicted biotransformation and generic LC peak-finding) for mining possible metabolites. LC peak, MS, and MS/MS intensity thresholds were set at 500, 100 and 50 cps, respectively.

Analysis of authentic human urine specimens

Two urine samples collected from individuals suspected of driving under the influence of drugs were provided by the National Board of Forensic Medicine in Linköping, Sweden. These two specimens were not from human experimental investigations. Specimens were anonymized and de-identified before shipping to our laboratory for analysis. These specimens are exempt from the institutional review board approval as they are anonymized and do not fall under human experimental investigations. The corresponding blood samples of the two urine samples were positive for NM-2201.

Urine samples were prepared both with and without enzymatic hydrolysis. β-Glucuronidase hydrolysis was performed as described previously, with slight modifications [19, 32]. Briefly, 250 µL urine was diluted with 600 µL ammonium acetate buffer (0.4 M, pH 4.0). β-Glucuronidase (40 µL, 15,625 IU/mL) was added and mixed; the mixture was then incubated at 55 °C for 1 h before being quenched by 200 µL acetonitrile. For non-enzymatic hydrolysis samples, 250 µL urine was diluted with 640 µL ammonium acetate buffer (0.4 M, pH 4.0) and 200 µL acetonitrile. After centrifugation (15,000×*g*, 4 °C, 5 min), all samples were loaded onto the Isolute SLE+ cartridges and eluted twice with 3 mL ethyl acetate. Extracts were dried at 45 °C under nitrogen, and reconstituted in 250 µL mobile phase A/B (80:20, *v*/*v*). A 25-µL volume of reconstituted solution was injected for analysis; data acquisition and processing were the same as for hepatocyte samples.

Results

Metabolic stability of NM-2201 in HLMs

In HLMs, the in vitro $T_{1/2}$ of NM-2201 was calculated as 8.0 ± 1.5 min; in vitro $CL_{int,\ micr}$ was 0.088 mL/min/mg, corresponding to an intrinsic clearance (CL_{int}) of 81.6 mL/min/kg after scaling to whole-liver-dimensions [33]. Without considering plasma–protein binding, and using a simplified Rowland's equation [30, 34], we calculated human CL_H of 16.1 mL/min/kg and ER of 0.80.

Analysis of NM-2201 and reference standards of three possible metabolites

Chromatographic and MS fragmentation of NM-2201 and three possible metabolites was first studied with reference standards, i.e., 5F-PI-COOH, 5′-OH-PI-COOH and PI-COOH pentanoic acid. The fragmentation patterns of major product ions were characterized based on accurate mass measurement, and were used to facilitate elucidation of potential metabolites. The three metabolites are supposed to be shared by NM-2201 and 5F-PB-22 (Fig. 1a, b) after ester hydrolysis, as shown previously [12].

NM-2201 with $[M + H]^+$ at *m/z* 376.1717 eluted at 9.60 min and showed product ions at *m/z* 144.0446, 171.0445, 206.1343, 232.1140 and 358.1611 (Fig. 2a, b). The base peak ion at *m/z* 232.1140 was generated by cleavage of the ester bond; further neutral loss of CO or the C_5H_9F chain led to *m/z* 206.1343 and 144.0446, respectively; *m/z* 171.0445 derived from a bond cleavage between the ester and the indole core.

5F-PI-COOH eluted at 6.06 min and displayed a protonated molecular ion at *m/z* 250.1250. It produced the characteristic product ions at *m/z* 118.0662, 130.0659/132.0816, 144.0450, 174.0552, 206.1344 and 232.1139 (Fig. 2c, d). The ions at *m/z* 232.1139 and 206.1344 were generated via neutral loss of H_2O or CO_2 from its precursor *m/z* 250.1246. The most intense ions at *m/z* 132.0816 and 118.0662 represent the indole core with or without α-methylene. Ion *m/z* 174.0552 was formed by cleavage of the α and β carbon–carbon bond; *m/z* 144.0450 represents the indole ring with the attached carbonyl group.

5′-OH-PI-COOH possessed the protonated ion at *m/z* 248.1289, with a retention time of 4.18 min. It yielded characteristic product ions at *m/z* 118.0663, 130.0658, 144.0449, 174.0556, 186.1281, 204.1399 and 230.1186 (Fig. 3e, f). 5′-OH-PI-COOH is the oxidative defluorination product of 5F-PI-COOH; this pathway has been frequently reported for ω-fluoropentyl chain-containing SCs [14, 35]. Fragmentation patterns were similar for 5′-OH-PI-COOH and 5F-PI-COOH. The ions at *m/z* 230.1186 and 204.1399 were generated via neutral loss of H_2O or CO_2 from its precursor *m/z* 248.1289. Other product ions were the same as those of 5F-PI-COOH.

PI-COOH pentanoic acid with $[M + H]^+$ at *m/z* 262.1079 eluted at 4.21 min and yielded characteristic product ions at *m/z* 118.0651, 144.0443, 156.0810, 172.1120, 200.1073, 218.1187 and 244.0973 (Fig. 3g, h). PI-COOH pentanoic acid is the further oxidation product of 5′-OH-PI-COOH. The peak ion *m/z* 244.0973 was from neutral loss of H_2O, and further loss of CO_2 took place, leading to *m/z* 200.1073. The ion *m/z* 144.0443 was the same as that from NM-2201 and 5F-PI-COOH; *m/z* 156.0810 and 172.1120 were generated from neutral loss of HCOOH and further loss of HCOOH (or CH_3COOH) from its precursor *m/z* 262.1079.

All of the above product ions were used as diagnostic ions for metabolite elucidation, as similar cleavage patterns could be expected in metabolites.

NM-2201 metabolites in human hepatocytes

In the 3-h hepatocyte incubation sample, nine phase I and four phase II metabolites were detected for NM-2201; the parent compound was absent (Fig. 3; Table 1). None of these metabolites were observed after incubating NM-2201 in the buffer for only 3 h, indicating that metabolite formation was enzyme-dependent. Table 1 lists all the metabolites with their metabolic pathways, retention times, detected *m/z*, mass errors, elemental composition, product ions and peak areas in the 3-h sample. Metabolites were labeled "M" in the order of retention time. An overview of the metabolic pathway is shown in Fig. 4. Detailed metabolite elucidation is explained below.

Ester hydrolysis

NM-2201 was extensively hydrolyzed via ester hydrolysis, generating M13 and 1-naphthol, which was identified in the form of naphthol glucuronide (M5, Fig. 4).

M13 displayed a protonated molecular ion $[M + H]^+$ at *m/z* 250.1242 and eluted at 6.06 min. Its product ion spectrum revealed fragments at *m/z* 118.0663, 130.0658/132.0816, 144.0450, 174.0550, 206.1345 and 232.1136 (Fig. 5i). M13 chromatographic and MS behaviors (i.e., retention time, product ions and relative ion ratios) were identical to 5F-PI-COOH reference standard (Fig. 2d). Therefore, M13 was assigned as 5F-PI-COOH.

M5 (naphthol glucuronide) eluted early, at 3.37 min, and produced fragments at *m/z* 115.0548, 127.0550 and 145.0648 (Fig. 5e). Product ion *m/z* 145.0648 was formed by neutral loss of 176.0327 (glucuronide); further loss of water led to *m/z* 127.0550. M5 (naphthol glucuronide) was also observed as a minor metabolite of FDU-PB-22 after ester hydrolysis [27].

M13 further hydroxylation or glucuronidation

The predominant metabolite M13 underwent further hydroxylation and/or glucuronidation, yielding ten metabolites (M1, M2, M4 and M6–M12).

Direct glucuronidation of M13 led to M11. M11 eluted at 4.64 min and revealed product ions at *m/z* 118.0663, 130.0656/132.0814, 144.0446, 174.0549, 206.1341, 232.1135, and 250.1241 (Fig. 5h). The product ion *m/z* 250.1241 was formed by neutral loss of glucuronide (−176.0317 Da) from precursor ion *m/z* 426.1558; other product ions were the same as those of M13, suggesting that M11 was a glucuronide of M13.

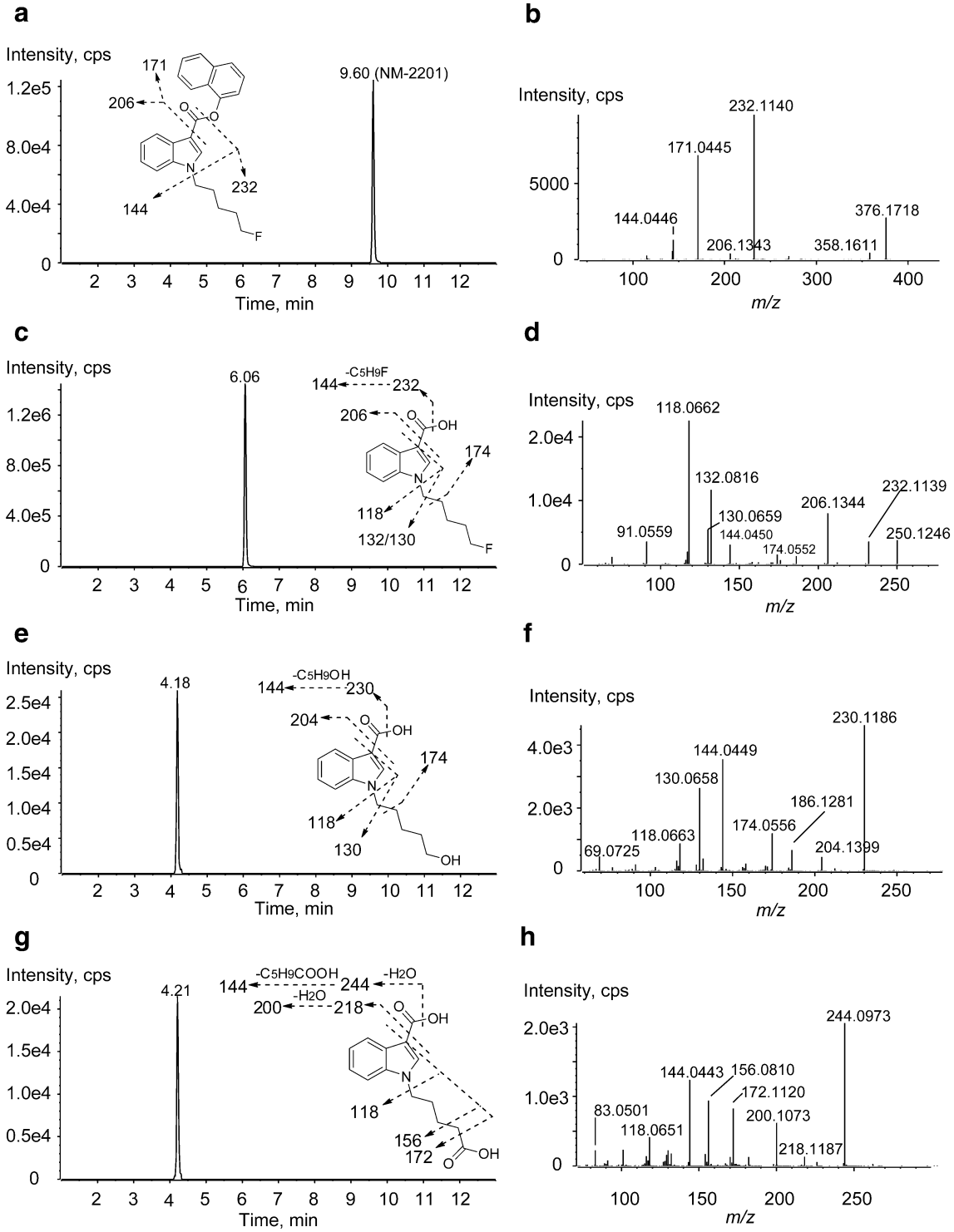

Fig. 2 Extracted ion chromatograms, corresponding product ion spectra and proposed fragmentation modes of reference standards NM-2201 (*m/z* 376.1703, **a**, **b**), 5-fluoro PB-22 3-carboxyindole metabolite (5F-PI-COOH; *m/z* 250.1250, **c**, **d**), PB-22 *N*-(5-hydroxypentyl)-3-carboxyindole metabolite (5′-OH-PI-COOH; *m/z* 248.1289, **e**, **f**), and PB-22 *N*-pentanoic acid-3-carboxyindole metabolite (PI-COOH pentanoic acid; *m/z* 262.1079, **g**, **h**)

Further metabolism of M13 generated six mono-hydroxylated and one di-hydroxylated metabolite. Among these, three were hydroxylated at the fluoropentyl chain (i.e., M2, M7, M9), three were hydroxylated on the indole moiety (i.e., M6, M10, M12), and the di-hydroxylated metabolite M1 was hydroxylated at both the fluoropentyl chain and indole moiety.

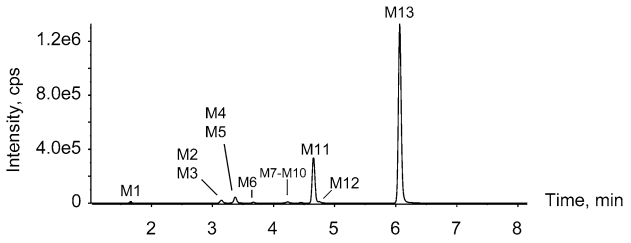

Fig. 3 Extracted ion chromatogram obtained by liquid chromatography–high-resolution mass spectrometry (LC–HR-MS) after processing by MetabolitePilot, showing metabolic profile of NM-2201 after 3-h incubation in human hepatocytes

M2, M7 and M9 showed precursor ions at *m/z* 266.1186 and shared similar product ions at *m/z* 118.0649, 130.0650/132.0813, 144.0437, 174.0548, 204.1177, 222.1283, and 248.1078 (Fig. 5b). Precursor ion *m/z* 266.1186 and product ions *m/z* 222.1283 and 248.1078 were 15.9944 Da (+O) larger than corresponding ions of M13 (5F-PI-COOH). Other product ions *m/z* 118.0649, 130.0650/132.0813, 144.0437, 174.0548 were the same as those of M13, indicating that the indole moiety was unmodified. Therefore, we propose that the hydroxylation is on the fluoropentyl chain.

M6, M10 and M12 displayed precursor ions at *m/z* 266.1187 and shared similar product ions at *m/z* 116.0521, 134.0600, 148.0758, 160.0367, 222.1285 and 248.1064 (Fig. 5f). Precursor ion *m/z* 266.1187 and product ions *m/z* 134.0600, 148.0758, 160.0367, 222.1285 and 248.1064 were 15.9945 Da (+O) larger than corresponding ions of M13 (5F-PI-COOH), indicating that the indole moiety was hydroxylated. Another ion *m/z* 116.0521 was generated from neutral loss of H_2O from *m/z* 134.0600.

The earliest-eluting metabolite, M1, is a di-hydroxylated metabolite of M13. M1 demonstrated a precursor ion at *m/z* 282.1131 and product ions at *m/z* 134.0560, 148.0760, 220.1188 and 264.1003 (Fig. 5a). Precursor ion *m/z* 282.1131 and product ion *m/z* 264.1003 were 31.9889 Da (+2O) larger than those of M13 (i.e., *m/z* 250.1242 and 232.1136), and product ions *m/z* 134.0560 and 148.0760 were 15.9957 Da (+O) larger than corresponding ions of M13 (5F-PI-COOH), indicating that the indole moiety was hydroxylated and that the other hydroxylation took place at the fluoropentyl chain.

M13 oxidative defluorination and sequential metabolism

Oxidative defluorination of M13 led to the formation of M8 ($[M + H]^+$ at *m/z* 248.1297). M8 eluted at 4.18 min and produced product ions at *m/z* 118.0638, 130.0639, 144.0437, 174.0556, 204.1381 and 230.1170 (Fig. 5g). Product ions *m/z* 204.1381 and 230.1170 were 1.9964 Da (+OH − F) less than corresponding ions of M13, indicating oxidative defluorination. Furthermore, M8 chromatographic and MS behaviors (i.e., product ions and retention time) were identical to the reference standard of 5′-OH-PI-COOH (Fig. 2f). Therefore, M8 is assigned as 5′-OH-PI-COOH.

Further oxidation and glucuronidation of M8 led to the formation of M4 ($[M + H]^+$ at *m/z* 438.1410). M4 eluted at 3.33 min and revealed product ions at *m/z* 130.0652/132.0808, 144.0437, 156.0810, 172.1120, 200.1051, 244.0972, and 262.0920 (Fig. 5d). Product ion *m/z* 262.0920 was produced by neutral loss of glucuronide from the precursor ion *m/z* 438.1410. All other product ions and ion abundance ratios were similar to those of PI-COOH pentanoic acid (Fig. 2h). Therefore, M4 was assigned as the glucuronide of PI-COOH pentanoic acid. PI-COOH pentanoic acid itself was not detected in the hepatocyte incubation samples.

N-Dealkylation and glucuronidation

All the above-mentioned metabolites were generated from extensive ester hydrolysis of NM-2201. We also observed a minor metabolite M3 without hydrolysis in the 3-h hepatocyte incubation sample. M3 eluted at 3.15 min, with the protonated molecular ion being *m/z* 464.1321. The product ion spectrum showed an intense ion at 288.1012 (Fig. 5c). Product ion *m/z* 288.1012 was 176.0325 Da (glucuronide) less than the precursor ion *m/z* 464.1337, and was also 88.0705 Da less than the protonated molecular ion of NM-2201 (*m/z* 376.1717), corresponding to loss of the C_5H_9F chain. Therefore, M3 was assigned as the glucuronide of *N*-dealkylated NM-2201.

Metabolite profiling in authentic urine specimens

In authentic human urine specimens, several metabolites were observed whereas the parent drug was not detected, suggesting that NM-2201 is highly metabolized in humans. As shown in Fig. 6a, c, three metabolites were identified in authentic urine 1 and 2 before hydrolysis, namely, M7, M11 and M13. Glucuronide conjugate M11 and its aglycone M13 (5F-PI-COOH) were the predominant metabolites.

After hydrolysis with β-glucuronidase, M11 disappeared, and the abundance of M13 increased significantly (Fig. 6b, d). This phenomenon further confirmed M11 as the glucuronide of M13 (Fig. 4). In addition to M13, three mono-hydroxylated metabolites M7, M9 and M12 were detected, at much lower abundance than M13. M9 and M12 were not detected before hydrolysis, likely because the MS signals of the glucuronides were low due to in-source fragmentation.

Table 1 Identification of NM-2201 metabolites after 3-h incubation with human hepatocytes

ID	Biotransformation	Retention time (min)	$[M + H]^+$ (*m/z*)	Mass error (ppm)	Formula	Fragment ions	Peak area	Rank
M1	5F-PI-COOH di-oxidation	1.67	282.1131	−1.9	$C_{14}H_{16}NO_4F$	134.0560, 148.0760, 264.1003	1.11E + 04	11
M2	5F-PI-COOH oxidation (fluoropentyl)	3.15	266.1186	−0.2	$C_{14}H_{16}NO_3F$	118.0649, 130.0650, 144.0437, 174.0548, 204.1177, 222.1283, 248.1078	4.38E + 04	4
M3	*N*-Dealkylation + glucuronidation	3.15	464.1321	−4.0	$C_{25}H_{21}NO_8$	288.1012	2.88E + 04	5
M4	5F-PI-COOH oxidative defluorination to carboxylic acid + glucuronidation	3.33	438.1410	0.7	$C_{20}H_{23}NO_{10}$	130.0652, 132.0808, 144.0437, 172.1120, 200.1051, 244.0972, 262.1076	9.35E + 03[a]	13
M5	Naphthol + glucuronidation	3.37	321.0975	2.0	$C_{16}H_{16}O_7$	115.0548, 127.0550, 145.0648	1.35E + 05[a]	3
M6	5F-PI-COOH oxidation (indole)	3.67	266.1187	−0.1	$C_{14}H_{16}NO_3F$	116.0521, 134.0600, 146.0601, 148.0758, 160.0367, 222.1285, 248.1064	1.86E + 04	9
M7	5F-PI-COOH oxidation (fluoropentyl)	4.10	266.1191	1.5	$C_{14}H_{16}NO_3F$	118.0640, 130.0669, 144.0466, 174.0550, 184.1146, 222.1292, 248.1078	2.15E + 04	8
M8	5F-PI-COOH oxidative defluorination	4.18	248.1297	6.2	$C_{14}H_{17}NO_3$	118.0638, 130.0639, 144.0437, 174.0556, 204.1381, 230.1170	1.05E + 04	12
M9	5F-PI-COOH oxidation (fluoropentyl)	4.23	266.1191	1.5	$C_{14}H_{16}NO_3F$	130.0646, 132.0815, 144.0412, 174.0552, 204.1135, 222.1277, 248.1052	2.76E + 04	6
M10	5F-PI-COOH oxidation (indole)	4.45	266.1181	−2.2	$C_{14}H_{16}NO_3F$	116.0499, 134.0597, 148.0768, 160.0404, 222.1288, 248.1126	1.34E + 04	10
M11	5F-PI-COOH glucuronidation	4.64	426.1558	−0.3	$C_{20}H_{24}NO_8F$	118.0663, 130.0656, 132.0814, 144.0446, 174.0549, 206.1341, 232.1135, 250.1241	1.05E + 06[a]	2
M12	5F-PI-COOH oxidation (indole)	4.75	266.1188	0.2	$C_{14}H_{16}NO_3F$	116.0523, 134.0594, 148.0763, 160.0391, 222.1273, 248.1096	2.20E + 04	7
M13	Ester hydrolysis to 5F-PI-COOH	6.06	250.1242	1.9	$C_{14}H_{16}NO_2F$	118.0663, 130.0658, 132.0816, 144.0450, 174.0550, 206.1345, 232.1136	4.36E + 06	1

ID identification, *5F-PI-COOH* 5-fluoro PB-22 3-carboxyindole

[a] Area of corresponding aglycone due to in-source fragmentation

Discussion

HLM metabolic stability

In the pharmaceutical industry, in vitro $T_{1/2}$ and CL_{int} estimate a drug's susceptibility to metabolism and assist in predicting in vivo hepatic clearance, in vivo half-life, and bioavailability [30]. Short $T_{1/2}$, high CL_{int} and estimated ER indicate that NM-2201 is a rapidly metabolized drug [33, 36]. HLMs are rich in carboxylesterases and cytochrome P450 oxidases [37]; the hydrolysis of NM-2201 was likely catalyzed by the liver carboxylesterases.

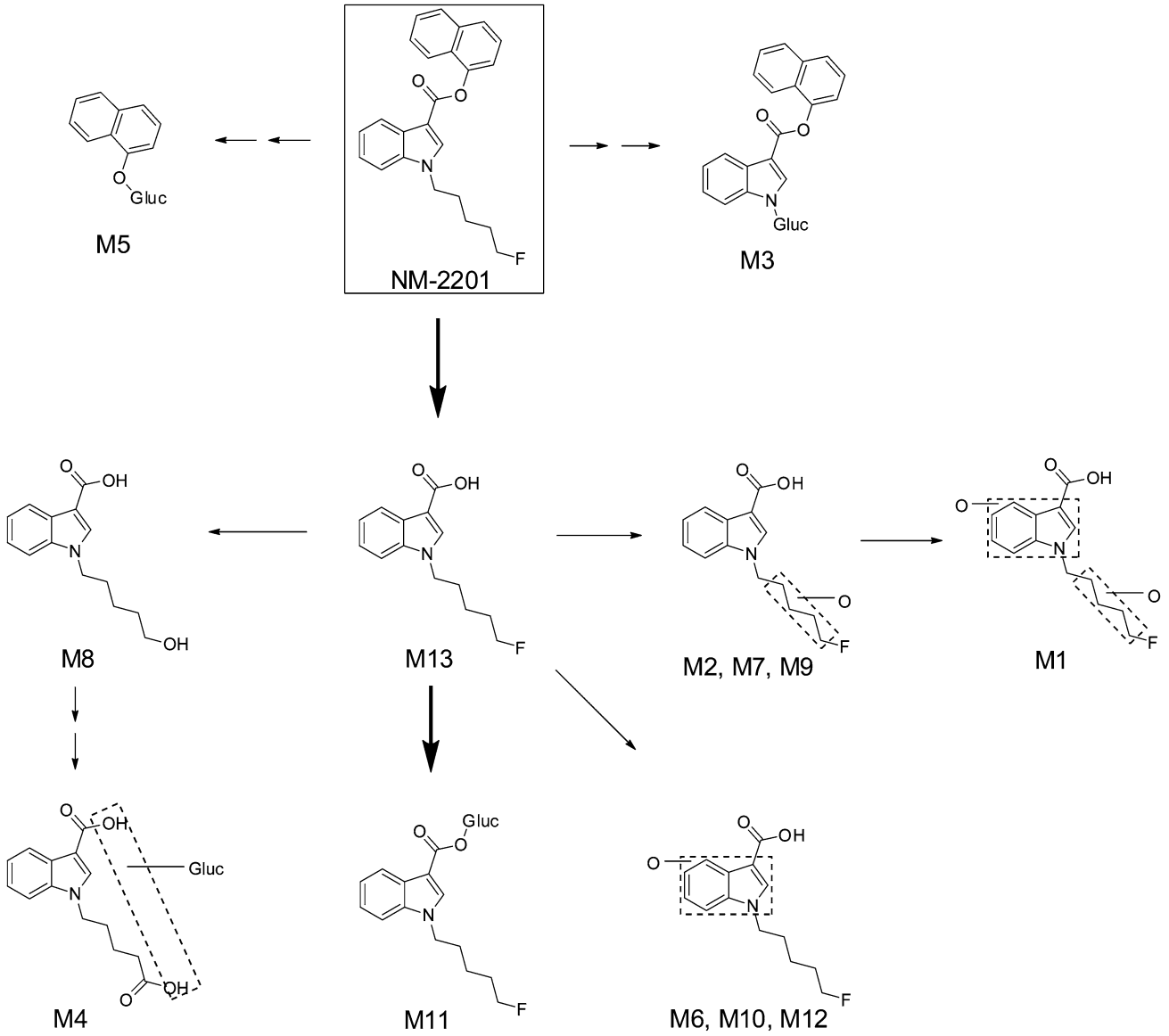

Fig. 4 Metabolic pathway of NM-2201 in human hepatocytes. *Gluc* glucuronide. *Bold arrows* indicate major pathways

Metabolism of NM-2201 compared to 5F-PB-22 and AM-2201

As shown in Fig. 1, NM-2201 and 5F-PB-22 possess quite similar substructures: an indole connects with naphthalene or quinoline via an ester bond. NM-2201 was significantly metabolized after 3-h incubation in hepatocytes. Ideally, intense metabolites that are specific for SCs should be targeted in forensic cases. In our study, however, it was not possible to identify a specific marker for NM-2201, because NM-2201 and 5F-PB-22 are rapidly hydrolyzed to the same primary metabolite, 5F-PI-COOH (M13), after losing essential components of the original structures. Though not perfect, 5F-PI-COOH appears to be the best target metabolite for NM-2201, based on our results. However, distinguishing the consumption of NM-2201 from 5F-PB-22 based on the detection of 5F-PI-COOH in human urine is challenging. NM-2201 generated a specific alcohol-conjugated metabolite M5 (naphthol glucuronide), which is not detected in 5F-PB-22. Unfortunately, the structures of M5 is too common and simple to serve as a representative marker of NM-2201, as it can also derive from other drugs of abuse (i.e., FDU-PB-22), medicine, or food supplements [38].

Previous studies have described oxidative defluorination and subsequent carboxylation as the major metabolic pathways for ω-fluoropentyl chain-containing drugs such as AM-2201 [22], 5F-AKB-48 [35], THJ-2201 [39], and

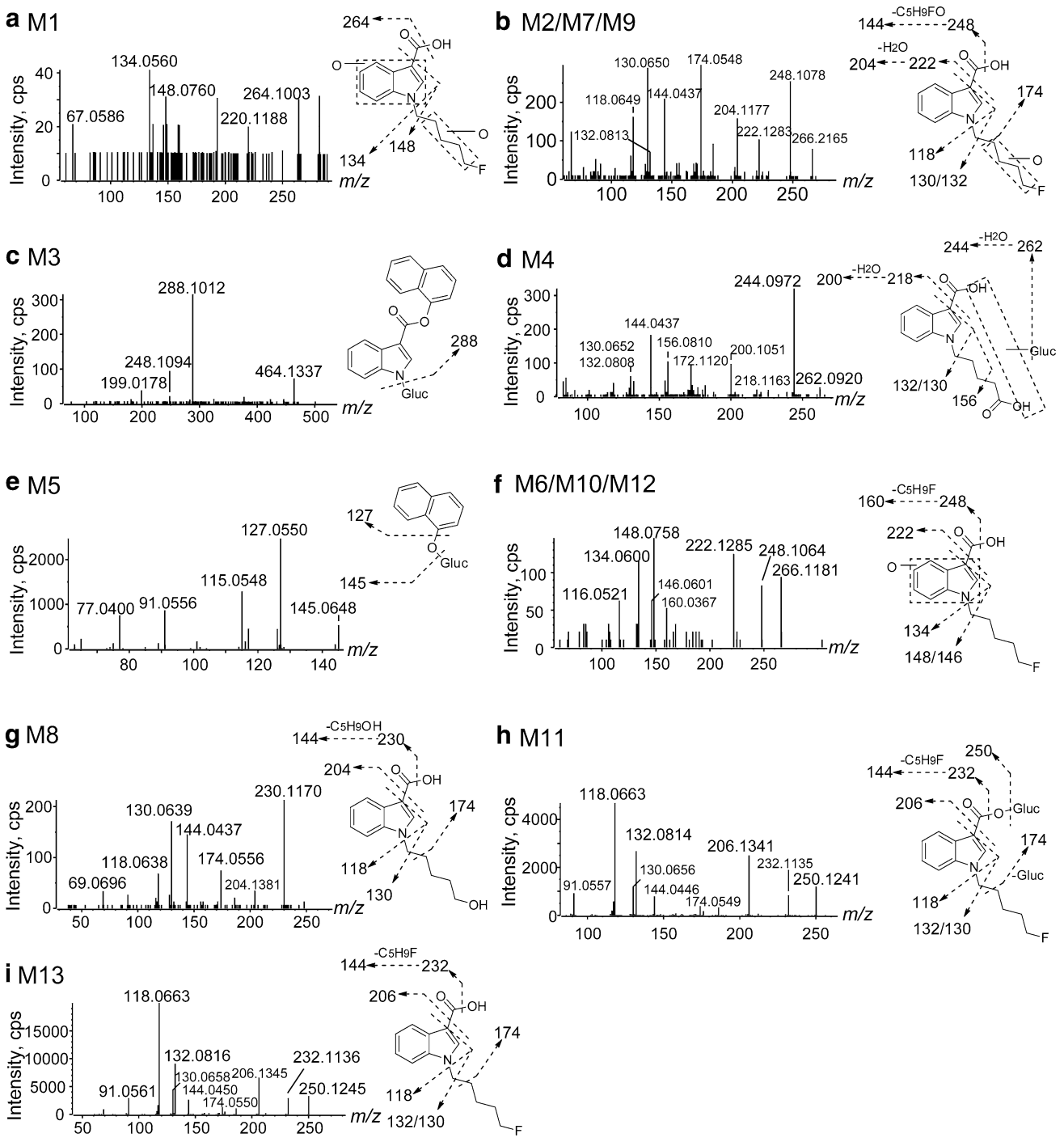

Fig. 5 Product ion spectra, proposed structures and fragmentation of NM-2201 metabolites. *Gluc* glucuronide

FUBIMINA [14]. In this study, however, although oxidative defluorination and carboxylation metabolites of 5F-PI-COOH (M13) were observed—i.e., M8 and M4—they were only minor metabolites compared to their abundance as metabolites of AM-2201, THJ-2201 and FUBIMINA. This was also observed in the metabolic profile of 5F-PB-22, where the hydrolysis metabolite 5F-PI-COOH was the predominant metabolite [12]. We thus conclude that SCs with an *N*-fluoropentyl indole (or indazole) connected to a naphthalene (or quinoline) via a carbonyl linkage do not generally undergo ester hydrolysis, but oxidative defluorination and subsequent carboxylation dominate metabolism. For SCs with *N*-fluoropentyl indole (or indazole) connected to naphthalene (or quinoline) via an ester bond linkage,

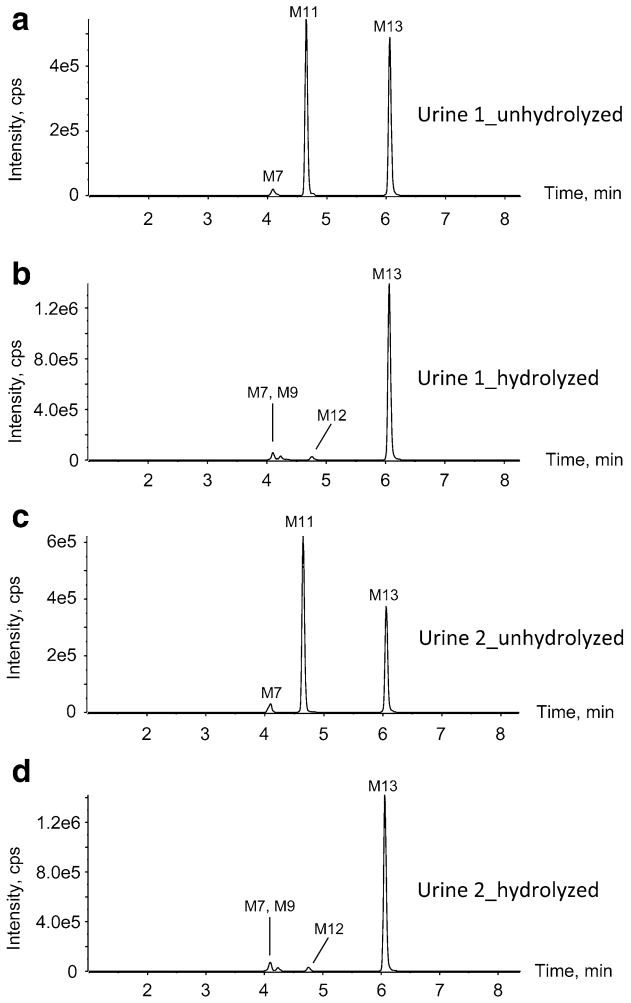

Fig. 6 Extracted ion chromatograms obtained by LC–HR-MS after processing by MetabolitePilot, showing metabolic profiles of NM-2201 in case urine 1 (**a**, unhydrolyzed; **b**, hydrolyzed) and case urine 2 (**c**, unhydrolyzed; **d**, hydrolyzed)

extensive ester hydrolysis takes place, while oxidative defluorination and subsequent carboxylation occur to only a minor extent after significant ester hydrolysis.

Urinary metabolites for documenting NM-2201 intake

Urine is a common matrix for drug detection and screening, given its non-invasive collection, adequate specimen volume, wider detection windows and higher drug concentrations than blood; however, the predominance of SC metabolites in urine [19, 22, 27] underscores the importance of identifying urinary metabolites. When extrapolating the hepatocyte metabolite profile to human urine, certain factors such as extrahepatic metabolism [40], kidney uptake or efflux transporters [41], metabolite enrichment in urine [42–44], and time intervals after drug consumption may affect the abundance ratios of urinary metabolites. Therefore, it is important to evaluate the metabolic profiles in real urine specimens, if available, to further document NM-2201 urinary markers.

In this study, we analyzed two urine specimens collected from individuals suspected of driving under the influence of drugs. The corresponding blood samples for urine samples 1 and 2 were positive for NM-2201. For both urine samples, four metabolites were detected after β-glucuronidase hydrolysis, namely, M13 (5F-PI-COOH), and three hydroxylated metabolites of M13 (M7, M9 and M12). Similar to the metabolic profile in the 3-h hepatocyte incubation sample, M13 was also found to be the predominant metabolite in both urine specimens. The three hydroxylated metabolites were present in quantities too small to be considered marker metabolites for NM-2201.

In some jurisdictions, unequivocal identification of a consumed substance is required for forensic testing, especially when identical metabolites may arise from a scheduled and non-scheduled compound. Therefore, metabolite M13 (5F-PI-COOH) is a good urinary marker to confirm consumption of NM-2201 and/or 5F-PB-22. However, it is not easy to distinguish NM-2201 from 5F-PB-22 intake based solely on urine results, because the same primary metabolite M13 is produced by extensive ester hydrolysis. Other metabolites derived from M13 were similar but present only as minor metabolites. As discussed above, M5 (naphthol) and quinolinol can derive from many origins, and their structures are too simple to be specific for NM-2201 or 5F-PB-22. Therefore, we cannot determine the specific SC consumed based only on the urine results. Definitive differentiation of NM-2201 from 5F-PB-22 intake would require identification of the parent compound in blood or oral fluid; however, the windows of detection of the potent parent compounds in these matrices are expected to be short due to their metabolic instability and low dosage.

Success of hepatocyte model in proposing urine marker metabolites

Despite higher costs, human hepatocytes offer many advantages over HLMs for identifying human metabolites of NPSs. Hepatocytes are more representative of the physiological liver environment containing all phase I and II drug-metabolizing enzymes, cofactors (such as NADPH) and drug transporters [25, 45]. In addition, compounds must penetrate cell membranes before being metabolized, which is not the case in HLMs. The hepatocyte model proved to be successful in confirming consumption of AB-FUBINACA [26], AB-PINACA [20], FDU-PB-22 and FUB-PB-22 [27]. In the current study, the primary

metabolite in hepatocytes, M13 (5F-PI-COOH), was also the dominant metabolite in clinical urine specimens after β-glucuronidase hydrolysis.

Our data will help clinical laboratories in targeting urinary markers of NM-2201 intake. These data also enable linkage of adverse events to specific SCs—in this case, to NM-2201. Our hepatocyte incubation and HR-MS analysis workflow is applicable to studies of newly emerging SCs.

Conclusions

This work represents the first reported characterization of in vitro and in vivo human metabolism of NM-2201. The hepatocyte model proved successful in determining major urinary metabolites. In authentic urine specimens, the parent drug was not detected; M13 (5F-PI-COOH) and M11 (the glucuronide of M13) were the primary metabolites. M11 was completely converted to M13 after β-glucuronidase hydrolysis. Thus, we propose M13 (5F-PI-COOH) as the best urinary marker for confirming NM-2201 consumption. However, we should note that 5F-PI-COOH is also a major metabolite of 5F-PB-22, which is a structural analog of NM-2201. Definitive differentiation of NM-2201 from 5F-PB-22 intake requires identification of the parent compound in the blood or oral fluid. Our data lay the foundation for future work by forensic and clinical scientists in developing analytical screening methods for identifying NM-2201 intake.

Acknowledgments This research is supported by the Intramural Research Program of the National Institute on Drug Abuse, National Institutes of Health. NM-2201 was generously donated by the US Drug Enforcement Administration. We also appreciate help from Dr. Ariane Wohlfarth in performing the HLMs metabolic stability assays.

Compliance with ethical standards

Conflict of interest The authors declare that they have no conflict of interest.

Ethical approval This article does not contain any studies with human participants or animals performed by any of the authors.

References

1. Auwärter V, Dresen S, Weinmann W, Müller M, Pütz M, Ferreiros N (2009) 'Spice' and other herbal blends: harmless incense or cannabinoid designer drugs? J Mass Spectrom 44:832–837
2. Namera A, Kawamura M, Nakamoto A, Saito T, Nagao M (2015) Comprehensive review of the detection methods for synthetic cannabinoids and cathinones. Forensic Toxicol 33:175–194
3. Pertwee RG (2006) Cannabinoid pharmacology: the first 66 years. Br J Pharmacol 147(Suppl 1):S163–S171
4. Huffman JW, Dai D, Martin BR, Compton DR (1994) Design, synthesis and pharmacology of cannabimimetic indoles. Bioorg Med Chem Lett 4:563–566
5. Cooper ZD (2016) Adverse effects of synthetic cannabinoids: management of acute toxicity and withdrawal. Curr Psychiatry Rep 18:52
6. Scheidweiler KB, Jarvis MJ, Huestis MA (2015) Nontargeted SWATH acquisition for identifying 47 synthetic cannabinoid metabolites in human urine by liquid chromatography-high-resolution tandem mass spectrometry. Anal Bioanal Chem 407:883–897
7. Hermanns-Clausen M, Kneisel S, Szabo B, Auwärter V (2013) Acute toxicity due to the confirmed consumption of synthetic cannabinoids: clinical and laboratory findings. Addiction 108:534–544
8. Seely KA, Lapoint J, Moran JH, Fattore L (2012) Spice drugs are more than harmless herbal blends: a review of the pharmacology and toxicology of synthetic cannabinoids. Prog Neuropsychopharmacol Biol Psychiatry 39:234–243
9. Forrester MB, Kleinschmidt K, Schwarz E, Young A (2012) Synthetic cannabinoid and marijuana exposures reported to poison centers. Hum Exp Toxicol 31:1006–1011
10. Young AC, Schwarz E, Medina G, Obafemi A, Feng SY, Kane C, Kleinschmidt K (2012) Cardiotoxicity associated with the synthetic cannabinoid, K9, with laboratory confirmation. Am J Emerg Med 30(1320):e1325–e1327
11. Ustundag MF, Ozhan Ibis E, Yucel A, Ozcan H (2015) Synthetic cannabis-induced mania. Case Rep Psychiatry 2015:310930. doi:10.1155/2015/310930
12. Wohlfarth A, Gandhi AS, Pang S, Zhu M, Scheidweiler KB, Huestis MA (2014) Metabolism of synthetic cannabinoids PB-22 and its 5-fluoro analog, 5F-PB-22, by human hepatocyte incubation and high-resolution mass spectrometry. Anal Bioanal Chem 406:1763–1780
13. Uchiyama N, Asakawa K, Kikura-Hanajiri R, Tsutsumi T, Hakamatsuka T (2015) A new pyrazole-carboxamide type synthetic cannabinoid AB-CHFUPYCA [*N*-(1-amino-3-methyl-1-oxobutan-2-yl)-1-(cyclohexylmethyl)-3-(4-fluorophenyl)-1*H*-pyrazole-5-carboxamide] identified in illegal products. Forensic Toxicol 33:367–373
14. Diao X, Scheidweiler KB, Wohlfarth A, Zhu M, Pang S, Huestis MA (2016) Strategies to distinguish new synthetic cannabinoid FUBIMINA (BIM-2201) intake from its isomer THJ-2201: metabolism of FUBIMINA in human hepatocytes. Forensic Toxicol. doi:10.1007/s11419-016-0312-2
15. Holm NB, Nielsen LM, Linnet K (2015) CYP3A4 mediates oxidative metabolism of the synthetic cannabinoid AKB-48. AAPS J 17:1237–1245
16. Chimalakonda KC, Seely KA, Bratton SM, Brents LK, Moran CL, Endres GW, James LP, Hollenberg PF, Prather PL, Radominska-Pandya A, Moran JH (2012) Cytochrome P450-mediated oxidative metabolism of abused synthetic cannabinoids found in K2/Spice: identification of novel cannabinoid receptor ligands. Drug Metab Dispos 40:2174–2184
17. Shevyrin V, Melkozerov V, Nevero A, Eltsov O, Baranovsky A, Shafran Y (2014) Synthetic cannabinoids as designer drugs: new representatives of indol-3-carboxylates series and indazole-3-carboxylates as novel group of cannabinoids. Identification and analytical data. Forensic Sci Int 244:263–275
18. Kondrasenko AA, Goncharov EV, Dugaev KP, Rubaylo AI (2015) CBL-2201. Report on a new designer drug: napht-1-yl 1-(5-fluoropentyl)-1H-indole-3-carboxylate. Forensic Sci Int 257:209–213
19. Castaneto MS, Wohlfarth A, Pang S, Zhu M, Scheidweiler KB, Kronstrand R, Huestis MA (2015) Identification of AB-FUBINACA metabolites in human hepatocytes and urine using high-resolution mass spectrometry. Forensic Toxicol 33:295–310
20. Wohlfarth A, Castaneto MS, Zhu M, Pang S, Scheidweiler KB, Kronstrand R, Huestis MA (2015) Pentylindole/pentylindazole

synthetic cannabinoids and their 5-fluoro analogs produce different primary metabolites: metabolite profiling for AB-PINACA and 5F-AB-PINACA. AAPS J 17:660–677
21. www.bluelight.org (2016) http://www.bluelight.org/vb/threads/721477-Any-Information-about-NM-2201. Accessed 28 April, 2016
22. Sobolevsky T, Prasolov I, Rodchenkov G (2012) Detection of urinary metabolites of AM-2201 and UR-144, two novel synthetic cannabinoids. Drug Test Anal 4:745–753
23. Andersson M, Diao X, Wohlfarth A, Scheidweiler KB, Huestis MA (2016) Metabolic profiling of new synthetic cannabinoids AMB and 5F-AMB by human hepatocyte and liver microsome incubations and high-resolution mass spectrometry. Rapid Commun Mass Spectrom 30:1067–1078
24. Diao X, Pang X, Xie C, Guo Z, Zhong D, Chen X (2014) Bioactivation of 3-n-butylphthalide via sulfation of its major metabolite 3-hydroxy-NBP: mediated mainly by sulfotransferase 1A1. Drug Metab Dispos 42:774–781
25. Soars MG, McGinnity DF, Grime K, Riley RJ (2007) The pivotal role of hepatocytes in drug discovery. Chem-Biol Interact 168:2–15
26. Castaneto MS, Wohlfarth A, Pang SK, Zhu MS, Scheidweiler KB, Kronstrand R, Huestis MA (2015) Identification of AB-FUBINACA metabolites in human hepatocytes and urine using high-resolution mass spectrometry. Forensic Toxicol 33:295–310
27. Diao X, Scheidweiler KB, Wohlfarth A, Pang S, Kronstrand R, Huestis MA (2016) In vitro and in vivo human metabolism of synthetic cannabinoids FDU-PB-22 and FUB-PB-22. AAPS J 18:455–464
28. Wang P, Zhao Y, Zhu Y, Sun J, Yerke A, Sang S, Yu Z (2016) Metabolism of dictamnine in liver microsomes from mouse, rat, dog, monkey, and human. J Pharm Biomed Anal 119:166–174
29. Ellefsen KN, Wohlfarth A, Swortwood MJ, Diao X, Concheiro M, Huestis MA (2016) 4-Methoxy-α-PVP: in silico prediction, metabolic stability, and metabolite identification by human hepatocyte incubation and high-resolution mass spectrometry. Forensic Toxicol 34:61–75
30. Baranczewski P, Stanczak A, Sundberg K, Svensson R, Wallin A, Jansson J, Garberg P, Postlind H (2006) Introduction to in vitro estimation of metabolic stability and drug interactions of new chemical entities in drug discovery and development. Pharmacol Rep 58:453–472
31. Swortwood MJ, Carlier J, Ellefsen KN, Wohlfarth A, Diao X, Concheiro-Guisan M, Kronstrand R, Huestis MA (2016) *In vitro*, *in vivo* and *in silico* metabolic profiling of α-pyrrolidinopentiothiophenone, a novel thiophene stimulant. Bioanalysis 8:65–82
32. Wang P, Chen H, Sang S (2016) Trapping methylglyoxal by genistein and its metabolites in mice. Chem Res Toxicol 29:406–414
33. McNaney CA, Drexler DM, Hnatyshyn SY, Zvyaga TA, Knipe JO, Belcastro JV, Sanders M (2008) An automated liquid chromatography-mass spectrometry process to determine metabolic stability half-life and intrinsic clearance of drug candidates by substrate depletion. Assay Drug Dev Technol 6:121–129
34. Diao X-X, Zhong K, Li X-L, Zhong D-F, Chen X-Y (2015) Isomer-selective distribution of 3-n-butylphthalide (NBP) hydroxylated metabolites, 3-hydroxy-NBP and 10-hydroxy-NBP, across the rat blood-brain barrier. Acta Pharmacol Sin 36:1520–1527
35. Vikingsson S, Josefsson M, Green H (2015) Identification of AKB-48 and 5F-AKB-48 metabolites in authentic human urine samples using human liver microsomes and time of flight mass spectrometry. J Anal Toxicol 39:426–435
36. Lave T, Dupin S, Schmitt C, Valles B, Ubeaud G, Chou RC, Jaeck D, Coassolo P (1997) The use of human hepatocytes to select compounds based on their expected hepatic extraction ratios in humans. Pharmaceut Res 14:152–155
37. Thomsen R, Nielsen LM, Holm NB, Rasmussen HB, Linnet K (2015) Synthetic cannabimimetic agents metabolized by carboxylesterases. Drug Test Anal 7:565–576
38. Michael JP (1999) Quinoline, quinazoline and acridone alkaloids. Nat Prod Rep 16:697–709
39. Diao X, Wohlfarth A, Pang S, Scheidweiler KB, Huestis MA (2016) High-resolution mass spectrometry for characterizing the metabolism of synthetic cannabinoid THJ-018 and its 5-fluoro analog THJ-2201 after incubation in human hepatocytes. Clin Chem 62:157–169
40. Li XD, Xia SQ, Lv Y, He P, Han J, Wu MC (2004) Conjugation metabolism of acetaminophen and bilirubin in extrahepatic tissues of rats. Life Sci 74:1307–1315
41. Gao C, Zhang H, Guo Z, You T, Chen X, Zhong D (2012) Mechanistic studies on the absorption and disposition of scutellarin in humans: selective OATP2B1-mediated hepatic uptake is a likely key determinant for its unique pharmacokinetic characteristics. Drug Metab Dispos 40:2009–2020
42. Xie C, Zhou J, Guo Z, Diao X, Gao Z, Zhong D, Jiang H, Zhang L, Chen X (2013) Metabolism and bioactivation of famitinib, a novel inhibitor of receptor tyrosine kinase, in cancer patients. Br J Pharmacol 168:1687–1706
43. Gao R, Li L, Xie C, Diao X, Zhong D, Chen X (2012) Metabolism and pharmacokinetics of morinidazole in humans: identification of diastereoisomeric morpholine N^+-glucuronides catalyzed by UDP glucuronosyltransferase 1A9. Drug Metab Dispos 40:556–567
44. Li Y, Wang K, Jiang Y-Z, Chang X-W, Dai C-F, Zheng J (2014) 2,3,7,8-Tetrachlorodibenzo-*p*-dioxin (TCDD) inhibits human ovarian cancer cell proliferation. Cell Oncol 37:429–437
45. Li AP, Gorycki PD, Hengstler JG, Kedderis GL, Koebe HG, Rahmani R, de Sousas G, Silva JM, Skett P (1999) Present status of the application of cryopreserved hepatocytes in the evaluation of xenobiotics: consensus of an international expert panel. Chem-Biol Interact 121:117–123